Biomass Conversion and Biorefinery (2024) 14:2439–2452
https://doi.org/10.1007/s13399-022-02382-8

ORIGINAL ARTICLE

Synthesis of polyamide grafted on biosupport as polymeric adsorbents for the removal of dye and metal ions

Osamah A. Bin-Dahman[1] · Tawfik A. Saleh[2]

Received: 26 November 2021 / Revised: 19 January 2022 / Accepted: 20 January 2022 / Published online: 4 February 2022

Abstract

The polymeric composite adsorbent was successfully synthesized by grafting polyamide on eggshell (CMP). The performance of the CMP composite as an adsorbent was studied for the methylene blue (MB) dye removal in a batch mode system. The effects of several factors such as adsorbent dosage, initial concentration of MB dye, and initial solution pH on the efficiency of MB removal were investigated. Kinetic studies were implemented to understand the adsorption mechanism. The maximum adsorption capacity was achieved under the conditions of an initial concentration of 200 ppm, the adsorbent dosage of 0.01 mg, and solution pH of 6 at room temperature. The pseudo-second-order kinetic model showed best fitted the experimental data. The adsorption capacity of the CMP was 345 ± 4 mg/g at 298 K for MB dye. The adsorption mechanisms included π-π interactions, electrostatic attraction, interaction with functional groups, and formation of complexes. The CMP showed simultaneous removal of MB dye and toxic metals such as Pb, Cr, Ni, Cd, Hg, and As. The CMP composite can be potentially used as an efficient and low-cost biosorbent for the removal of MB dye and heavy metals.

Keywords Water treatment · Polymer · Removal · Adsorption · Sustainability · Green technology

1 Introduction

Water contamination is a major worldwide environmental problem owing to its serious global threat to living organisms as well as to the equilibrium of the entire ecosystem.

A large variety of toxic pollutants such as synthetic dyes and heavy metals are dumped into water sources from various chemical industries and everyday activities. Dyes are resistant to biodegrade owing to their stability and have harsh effects on human health because of their toxic nature. Methylene blue dye, for example, can cause skin-related problems at a lower dose (2–4 mg/kg) [1]. Furthermore, the mixing of organic dyes with water may alter its quality and cause the death of aquatic organisms [2]. Exposure to heavy metal ions such as lead (Pb), nickel (Ni), mercury (Hg), zinc (Zn), cobalt (Co), cadmium (Cd), copper (Cu), and chromium (Cr) can cause a wide spectrum of health problems for human and animals. These metals can bind to proteins, nucleic acids, and metabolites, and change or loss biological tasks such as inhibition of enzymes, blockade heme biosynthesis, or accumulation in bones [3].

Several water treatment techniques have been applied to remove harmful contaminants from the polluted water including ion exchange, reverse osmosis, and chemical precipitation [4]. However, these methods are too expensive and considered insufficient to treat water pollutants due to their limited effectiveness for the removal of dyes from wastewater in addition to high operational costs [5, 6].

The adsorption process is currently considered to be one of the best useful methods in purification processes and to be the most effective and economical process [7, 8]. Numerous adsorbents have been investigated for the removal of pollutants from water such as clay minerals, activated carbon, fly ash, titanium oxide, carbon nanotubes, and graphene oxide [9–14]. However, these adsorbents have a few drawbacks that limited their use like high cost, and some adsorbents are difficult to be recovered from the aquatic system when the effluent reaches the maximum permissible discharge level [15].

Recently, more efficient bio-adsorbent derived from solid waste or low-cost materials have been used in water

✉ Tawfik A. Saleh
tawfikas@hotmail.com; tawfik@kfupm.edu.sa

[1] Department of Chemical Engineering, College of Engineering and Petroleum, Hadhramout University, Mukalla, Hadhramout, Yemen

[2] Department of Chemistry, King Fahd University of Petroleum and Minerals, Dhahran 31261, Saudi Arabia

treatment processes [16]. Some alternative adsorbents have been reported in literature include the orange peel [17], chitosan [18], banana peel, grape pomace [19], eggshell [20], coffee residues [21], rice straw [22], olive stones [23], artichoke agrowaste [24], sugarcane bagasse [25], and bamboo shell [26]. The development of adsorbents which have superior properties such as high mechanical strength, fast adsorption rate, and excellent adsorption capacity, has attracted great attention in wastewater treatment technologies.

Eggshells are abundantly obtainable and have been extensively investigated for their utilization towards a wide variety of applications such as promising biomaterials for bone graft substitutes [27], heterogeneous catalysts for biodiesel production [28], cement productions [29], and plant fertilizer [30]. Eggshell (ES) is made almost entirely of calcium carbonate ($CaCO_3$) crystals, which form more than 90% of the dry ES [31]. Chicken eggshell is the by-product of the food industry and causes a big waste disposal problem, but it has excellent mechanical properties, which gives reason to be considered as a good adsorbent [32]. Due to its porous structure and surface properties, eggshell has been broadly applied for the removal of various pollutants from water such as heavy metals and chemical dyes, making it a promising natural bio-adsorbent [31, 33]. Eggshell has been effectively used in removing numerous contaminants with the removal efficiency observed in the range of 94–98% [34].

Several approaches have been reported to convert eggshell waste into useful material for the removal of chemical dyes and heavy metal ions from contaminated water [15, 35]. Polymers are considered favorable adsorbents because of their promising mechanical properties, modifiable surface chemistry, desirable pore size distribution, high surface area, practical regeneration under mild conditions, and selectivity for purification [36, 37].

Recent research in this area has concentrated on polymers and their modification with different bio-adsorbents such as chitosan [38], starch [39], and guar gum [40] to improve their properties as attractive adsorbents. The incorporation of polymeric materials offers extra active sites for adsorption and increases the surface area of the adsorbents [41]. Polymers having mercapto, imino, and amino groups are of great interest due to their good selectivity to heavy metal ions and outstanding adsorption capacity [37].

In the present study, a polymer composite adsorbent was prepared by grafting polyamide on eggshells. The feasibility of the prepared adsorbent for the effective removal of methylene blue dye from aqueous solutions under batch conditions was investigated. Moreover, the simultaneous adsorption of methylene blue dye and metal ions in a real water sample was studied. The prepared polymer composite adsorbent showed high adsorption capacity for the removal of methylene blue dye from water as well as for the simultaneous removal of metal ions and MB dye from real water.

2 Experimental

2.1 Reagents and equipment

Trimesoyl chloride (TMC; $C_6H_3(COCl)_3$, molecular weight 265.48 g/mol, purity ≥ 99%), methylene blue dye (MB: molecular weight: 319.85; $C_{16}H_{18}ClN_3S$; reagent grade), and m-phenylenediamine (MPD: molecular weight: 108.14; C_6H_4-1,3-$(NH_2)_2$), were supplied from Sigma-Aldrich. Hexane solvent ($CH_3(CH_2)_4CH_3$; assay:95%) was provided by Merck Company. Standard solutions of metal oxides were obtained from Sigma-Aldrich. One thousand mg L^{-1} stock solution was prepared in distilled water and then diluted and used when needed for testing. The pH measurement was conducted using a pH meter (Sartorius pp-15, Germany).

2.2 Preparation

Eggshells were crushed using a pulverizer and dried in a vacuum furnace with nitrogen flow at 120 °C for 3 h. Then the obtained powder was dispersed in a 2% (w/v) solution of m-phenylenediamine in water. The system was kept under sonication for 3 h. After that, 0.1% (w/v) trimesoyl chloride in n-hexane solution was added dropwise into the dispersed components under vigorous stirring for 2 h. The system was then transferred into the reflux system and kept under stirring for 24 h at 90 °C. Then, the obtained calcium carbonate particles modified with polyamide composite (CMP) were separated and washed several times, Fig. 1. Then it was dried in a freeze dryer.

2.3 Characterization

Fourier transform infra-red (FTIR) spectroscopy (Smart iTR NICOLET iS10) was used to characterize the functional groups present on both the eggshell powder and modified shells with polyamide. Scanning electron microscope (SEM) was performed to study their surface morphology. An ultrathin layer of gold was applied to the prepared samples prior to the SEM analysis to produce an electrical conductivity on them. An energy dispersive x-ray spectrometer (EDX, Oxford Instruments) was utilized for the elemental studies. X-ray mapping was applied to represent the distribution of the elements on the surface of the materials. Inductively coupled plasma-atomic emission spectroscopy (ICP-AES) (PlasmaQuant® PQ 9000) was used for the metal ions analysis. The initial and final MB concentrations were monitored using a UV/vis (Thermo Scientific™ GENESYS™ 10S) Spectrophotometer at λ_{max} of 664 nm. Furthermore, the surface area and the average pore size distribution were measured using a TriStar II PLUS, from Micromeritics Co., GA, USA.

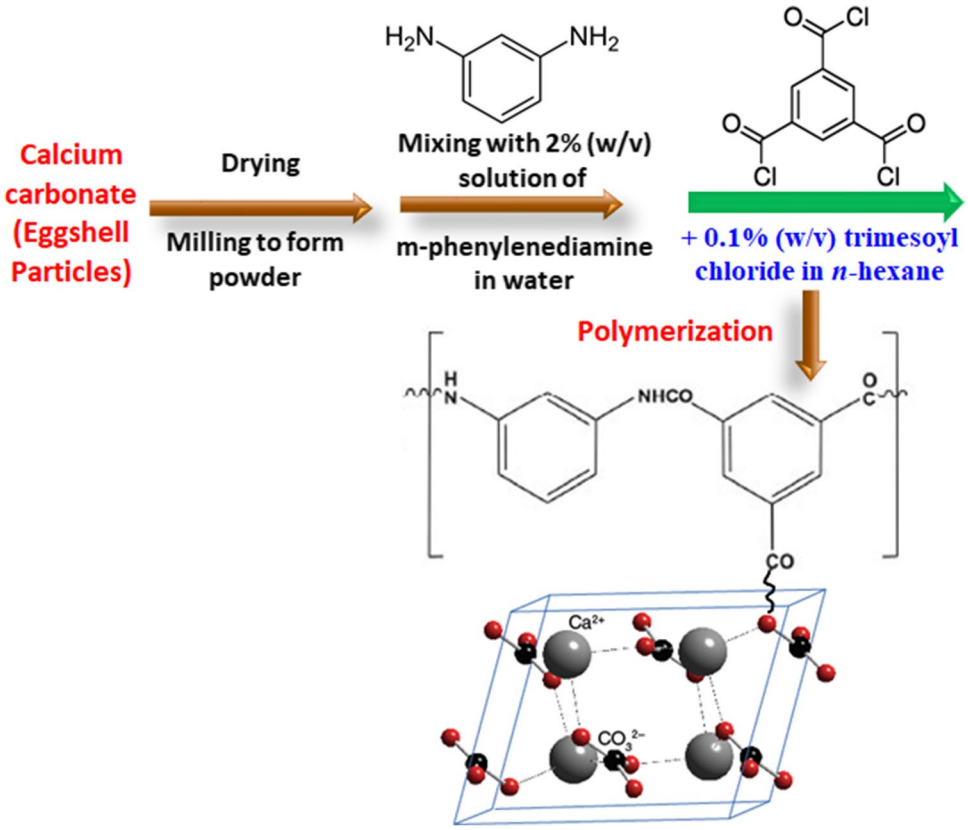

Fig. 1 Scheme for the synthesis of eggshells grafted with polyamide (CMP)

2.4 Adsorption tests

Adsorption experiments were carried out with optimization to the related conditions, adsorbent dosage, solution pH, contact time, and temperature. Model solution of the pollutant was used. Experiments were performed in triplicate and average was considered to calculate % removal as follows:

The percentage removal of MB dye at equilibrium was calculated using the following equation:

$$\text{Removal } \% = \frac{(C_i - C_e)}{C_i} \times 100 \tag{1}$$

The capacities of adsorption were evaluated by the following two equations:

$$q_t = (C_i - C_t) \times \frac{V}{m} \tag{2}$$

$$q_e = (C_i - C_e) \times \frac{V}{m} \tag{3}$$

where C_i and C_e refer to the initial and equilibrium concentrations of MB dye (mg L^{-1}), respectively. C_t refers to the MB dye concentrations at any time t (mg L^{-1}). V represents the volume of dye solution (L), while m denotes the mass of the adsorbent (mg). q_e and q_t refer to the adsorption capacities of the prepared composite at an equilibrium state and at time t(mg g^{-1}), respectively. As a control sample, a blank experiment was carried out using MB dye solutions without adding materials.

2.5 Kinetic studies

Three kinetic models, pseudo-first-order, second-order model, and intraparticle diffusion, were applied to study the adsorption mechanisms and potential rate-controlling stage of MB dye on the synthesized composite. The linear form of Lagergren's equation for pseudo-first-order kinetics is given by Eq. (4) [42]:

$$\ln (q_e - q_t) = \ln\ q_e - k_1 t \tag{4}$$

where q_e and q_t (mg/g) are the adsorption capacities at equilibrium and at time t (min), respectively, k_1 (min^{-1}) denotes the constant of the first-order rate. The linear form of the Ho and McKay rate equation for pseudo-second-order kinetics can be described by Eq. (5) [43]:

$$\frac{t}{q_t} = \frac{1}{k_2 q_e^2} + \frac{t}{q_e} \tag{5}$$

where k_2(g/mg.min) designates the constant of second-order rate. It is necessary to fit the adsorption data to the intraparticle diffusion model to further understand the adsorption process and to distinguish the rate-determining step in the adsorption. This model is proposed based on the Weber and Morris theory and can be mathematically expressed by Eq. (6) [44]:

$$q_t = k_i t^{0.5} + C_i \quad (6)$$

where k_i stands for the intraparticle diffusion rate constant stage i (mg/g.min$^{1/2}$) and C_i is the intercept (mg/g). The linear line in the plot indicates the existence of an interparticle diffusion, and a higher *Ci* value implies a larger boundary effect.

2.6 Adsorption isotherm studies

To understand adsorption behaviors, it is essential to know how dye molecules are distributed between the liquid and solid phases at equilibrium. Three isothermal models, namely, Langmuir, Freundlich, and Tempkin, were applied to fit the experimental data. The linear form of the Langmuir isotherm model is given as [45]

$$\frac{C_e}{q_e} = \frac{1}{K_L.q_m} + \frac{C_e}{q_m} \quad (7)$$

where q_m is the maximum adsorption capacity (mg/g) and K_L is the Langmuir constant which denotes the binding affinity between the adsorbate and adsorbent (L/mg). q_e is the capacity of adsorption (mg/g), while and C_e is adsorbate concentration at equilibrium (mg/L). The values of K_L and q_m can be calculated from the intercept and slope of plot C_e/q_e against C_e. The separation factor (R_L) is given in Eq. (8) [46]:

$$R_L = \frac{1}{(1 + K_L.C_0)} \quad (8)$$

where C_0 is the dye initial concentration (mg/L). The R_L value specifies the type of isotherm to favorable ($0 < R_L < 1$), unfavorable ($R_L > 1$), linear ($R_L = 1$), or be irreversible ($R_L = 0$) [47]. The linear form of Freundlich isotherm model is given in Eq. (9) [48].

$$\ln\ q_e = \ln\ K_F + \frac{1}{n} \ln\ C_e \quad (9)$$

where K_F is Freundlich constant (mg/g) which expresses adsorption capacities. The value of 1/n defines the intensity of adsorption. The 1/n value specifies the type of isotherm to be irreversible ($1/n = 0$), favorable ($0 < 1/n < 1$), and unfavorable ($1/n > 1$) [47]. The linear equation of Temkin isotherm expression is [49]:

$$q_e = \frac{RT}{b_T} \ln\ K_T + \frac{RT}{b_T} \ln\ C_e \quad (10)$$

where K_T is the Temkin isotherm constant (L/g), while b_T is the equilibrium binding constant (J/mol). T and R are temperature and the gas constant, respectively.

3 Results and discussion

3.1 Characterization

The prepared eggshell powder and the polymer-modified eggshell composite (CMP) were characterized using FTIR, SEM, and EDX. The FTIR spectra of both eggshell and CMP composite were depicted in Fig. 2. The broad wavelength observed in the range of 3300–3500 cm^{-1} was assigned to N–H stretching vibration of 1,3 phenylenediamine [50]. The bands at around 2900 cm^{-1} and 2850 cm^{-1} were attributed to C–H stretching vibration. The band at 1628 cm^{-1} was attributed to C = O stretching vibration. The peaks in the range of 1600–1400 cm^{-1} were related to the C = C aromatic stretch. The typical C–O stretching bands were observed in the range 1200–1100 cm^{-1}.

SEM was used to provide insights on the morphology of eggshell powder and the polymer-modified eggshell composite (CMP) and the obtained SEM images were shown in Fig. 3a–b. The CMP composite has irregular shapes and sizes compared to eggshell powder. It is also clear that the CMP composite has rough surfaces with more pores of different sizes, which provides a large free surface area. It indicates a very good chance for MB dye to be adsorbed onto its surface. EDX analysis confirms that the main composition of the eggshell powder was calcium carbonate ($CaCO_3$). The elemental analysis of the CMP composite detected the presence of nitrogen and showed a relatively high percentage of carbon compared with eggshell powder. This can be attributed to the existence of functional groups of polyamide on the CMP surface which may enhance the adsorption. The surface area of the prepared CMP was 285 ± 7 m^2/ g, which is considered high and important for the adsorption of mercury ions. The average pore size distribution of the CMP was 5.3 ± 0.3 nm, and the total pore volume was 0.91 ± 0.2 cm^3/g. Consequently, the functionality and high surface area of the developed polymer adsorbent plays a key role in the adsorption efficiency.

3.2 Adsorption experiments

3.2.1 Effect of dosage of adsorbent

The effect of eggshell powder and CMP composite amount (0.001 to 0.08 g with 20 mL of 100 ppm initial dye solution at 25 °C) was examined with regard to the adsorption of MB dye under batch adsorption experiments (Fig. 4). As

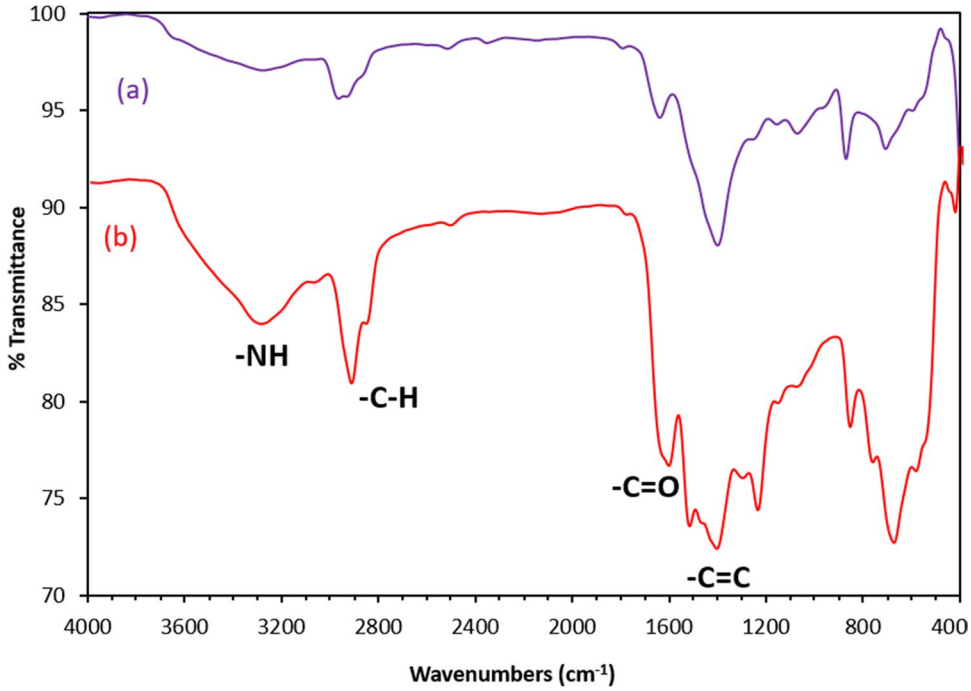

Fig. 2 FTIR of (**a**) the eggshell powder and (**b**) the prepared polyamide modified shell composite (CMP)

observed, the removal of MB increases with increasing the dosages of eggshell and CMP composite. However, the CMP composite shows a higher adsorption capacity towards MB compared to eggshell powder. The adsorption capacity dramatically increased from 0.001 to 0.04 mg/20 mL using the CMP composite. Increasing the amounts of CMP composite adsorbent caused an increase in the surface functional group density, and extra adsorption sites for the adsorbent became available, thus removing more of the dye molecules [51]. No effect of the CMP composite dosage was detected on MB removal from solution when the dosage of adsorbent increased from 0.04 to 0.08 mg/ 20 mL. As described in the literature, this means that the adsorption reaches equilibrium between MB molecules on the CMP composite and non-adsorbed MB molecules in the solution [52].

3.2.2 Effect of pH

The variations in pH values are a key factor for solute adsorption. These variations switch the ionization degree of the adsorbate and therefore change its surface properties. As a result, the adsorption capacity of the dye significantly depends on the pH of the solution [53]. Fig. 5 displays the variation of the adsorption capacity of MB on the surface of CMP at different pH values (dye volume = 20 mL, C_0 = 100 ppm, temperature = 298 K). As shown, the MB removal increases with increasing the initial pH of dye solution and then remains constant from 5.0 to 7.0. The maximum value of approximately 100% removal was achieved at a pH of 5. The measuring pKa value of MB is 3.8; for values below this pH value, MB is existing in the molecular form and has a positive charge above this value [54]. The MB molecules are generally neutral at pH lower than 3.8 and thus do not contribute to ionic/electrostatic interactions with the CMP. The adsorption of MB by the CMP at low pH could be attributed to hydrophobic, aromatic $\pi-\pi$ stacking, and hydrogen bond interactions [55, 56]. The structure of the shell membranes is primarily composed of protein and polysaccharides that contain functional groups such as hydroxyl, amine, and sulfonic groups [57]. Thus, the CMP composite has good adsorption characteristics owing to the availability of adsorption sites that may interact with the positive charges of MB. The improvement in MB adsorption removals at a higher solution pH ($pH > pKa_{,MB}$) could be described by the electrostatic attraction between the positive charges of MB and the negative charges of the CMP. The constant adsorption removal over the pH range 5 to 7 can be due to the adsorption of MB on the CMP controlled by both the electrostatic interaction and non-electrostatic contributions (such as hydrophobic interaction, hydrogen bonds, and van der Waals forces). This implies the adsorption of MB from aqueous solution by the CMP is a complex relation between electrostatic and non-electrostatic interactions [58].

3.3 Adsorption kinetics

Variations in the adsorption capacity (q_t) with contact time at different initial concentrations of dye ranging from 50

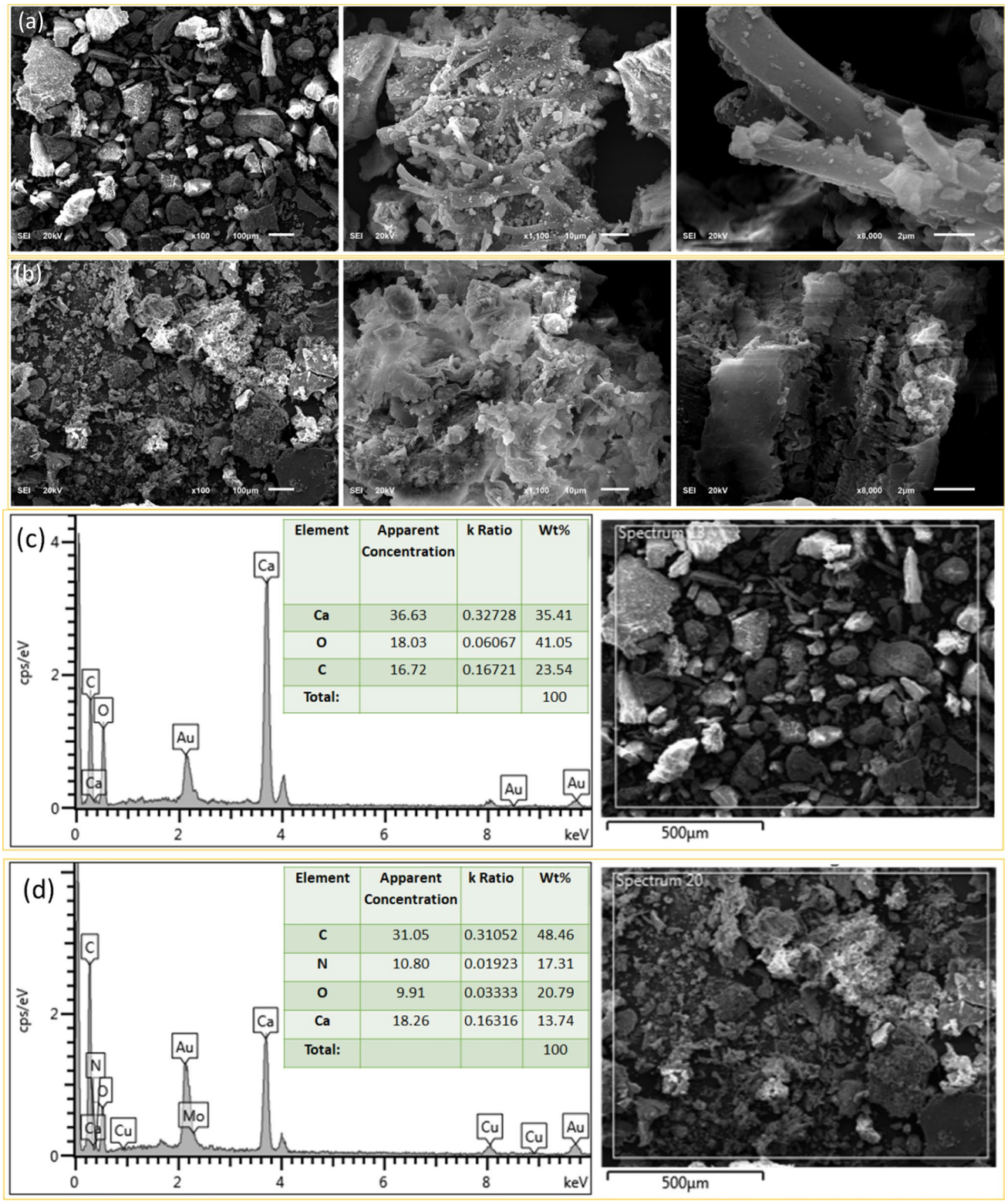

Fig. 3 SEM micrographs of (**a**) the eggshell powder and (**b**) the prepared polyamide modified shells (CMP) and (**c**) and (**d**) EDX spectra of the same

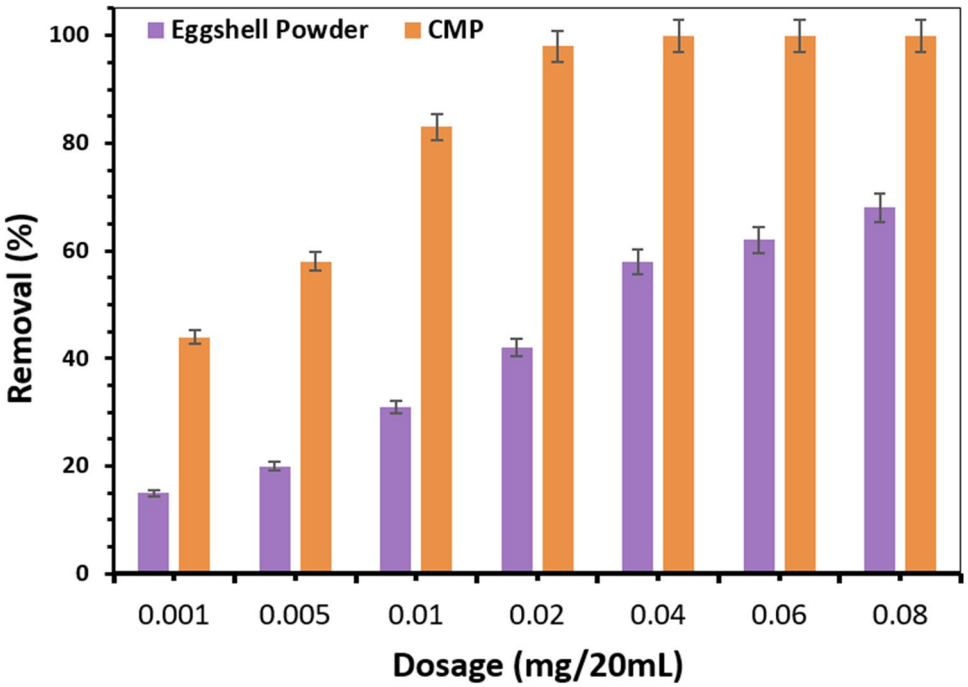

Fig. 4 Effect of adsorbent dosage on MB dye adsorption efficiencies by the eggshell powder and CMP composite (adsorption conditions: initial MB concentration = 100 ppm, solution volume = 20 mL, temperature = 298 K)

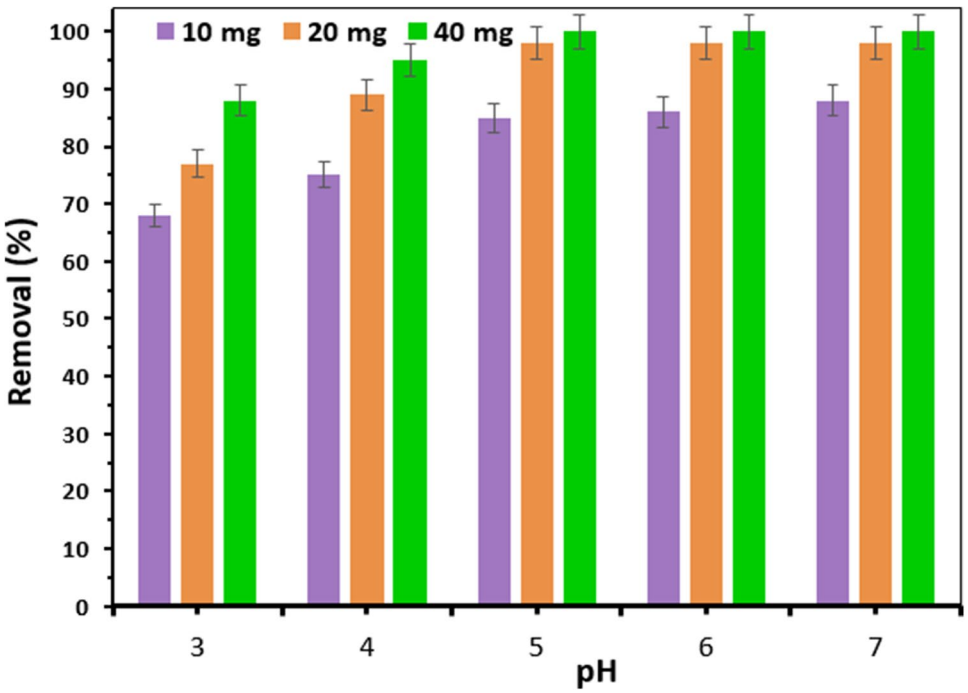

Fig. 5 Effect of initial pH on the adsorption removal of MB by CMP (initial MB concentration = 100 ppm, solution volume = 20 mL, temperature = 298 K)

to 200 ppm are shown in Fig. 6a. All the experiments were conducted at pH = 6, temperature = 298 K, and with a fixed amount of adsorbent (0.01 mg). A similar trend was detected for the adsorption of dye for all the concentrations, where an initial fast adsorption phase proceeded to a slower adsorption phase until the equilibrium was reached. The existence of a fast adsorption phase at the initial stage is probably due to the abundant adsorption sites on the CMP that are accessible for interaction with dye molecules in the solution. With a further increase of time, the number of active sites accessible for the adsorption process decreased, which leads to a slower increase in the adsorption rate [59]. In the equilibrium, the quantity of adsorbed dye and the quantity of dye desorbed were in dynamic equilibrium [60]. At low concentration (50 ppm), the adsorption was fast, and the equilibrium was achieved after 60 min of contact. At high

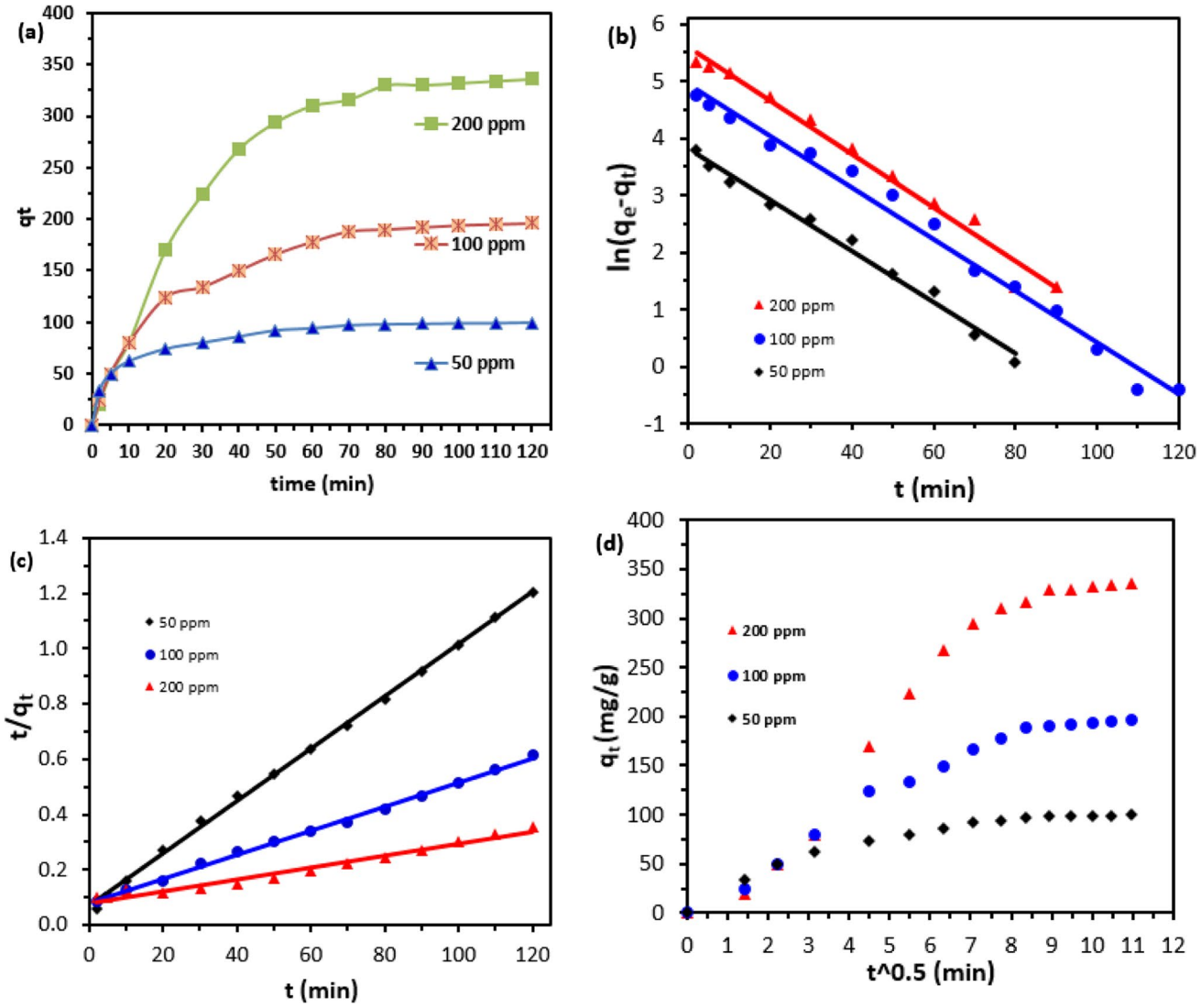

Fig. 6 **a** Adsorption capacity as a function of time at different initial MB concentrations, (**b**) pseudo-first-order model, (**c**) pseudo-second-order model, (**d**) intraparticle diffusion; dosage = 0.01 mg, temperature = 298 K, pH = 6

concentrations of dye (> 50 ppm), the adsorption was slower than at low concentrations and take more time to reach the equilibrium.

There are different mechanisms involved in the adsorption process such as adsorption surface, mass transfer, and intraparticle diffusion. In this study, three kinetic models, namely pseudo-first-order, pseudo-second-order, and intraparticle diffusion, are applied to analyze the experimental data obtained in the adsorption of MB dye onto the CMP. The fitting of experimental data to kinetic models is demonstrated in Fig. 6b, c, and d, and the main parameters for each kinetic model are listed in Table 1. The determination

Table 1 Parameters of kinetic models for MB dye at 298 K

C_i	q_e exp	Pseudo-first-order			Pseudo-second-order			Intraparticle diffusion		
		k_1	q_e(mg/g)	R^2	k_2	q_e(mg/g)	R^2	k_{id}	C	R^2
(mg/L)	(mg/g)	(min^{-1})	cal		(g/mg.min)	cal		(mg/g.min)	(mg/g)	
50	99.6	0.044	67	0.996	0.0014	105	0.989	0.9	0.7	0.998
100	196	0.045	211	0.987	0.0002	227	0.998	1.9	0.8	0.988
200	336	0.047	403	0.983	0.0001	455	0.997	3.2	1.1	0.987

of linear regression coefficient values (R^2) is crucial to determine the best fit kinetic models to the experimental data. Based on the comparison of the R^2 values, the pseudo-second-order model provides a better fit to experimental data than the pseudo-first-order model. These results indicate that the adsorption of MB dye onto CMP is controlled by chemisorption. Chemisorption takes place when strong interactions, such as hydrogen bonding and covalent and ionic bond formation, take place between adsorbate molecules and adsorbent surfaces. Similar findings were observed by Lin et al. in the adsorption of acid orange (AO7) and toluidine blue (TBO) dyes onto modified eggshell [36] and by El-Kemary et. al. in the adsorption of acid red nylon 57 (AN57) anionic dyes onto decorated eggshell [61].

Figure 6d shows the plots of the intraparticle diffusion model for MB dye adsorption. In this model, the adsorbed capacity at time t, q_t, was plotted versus the $t^{1/2}$, and the k_i and C_i parameters for the second stage were obtained, as shown in Table 1. The intraparticle diffusion model is applied to know whether external transport or intraparticle transport controls the rate of adsorption processes. As observed, three different separate regions can be distinguished in the plots for the range of concentrations investigated, indicating several stages of MB dye adsorption. The first region is connected to the external diffusion, while the second region represents the existence of intraparticle diffusion. At the third region, the intraparticle diffusion starts to diminish due to the low concentration of the adsorbed dye, and the equilibrium stage was obtained in this region. The linear lines of the second stage did not pass through the origin point because the final and initial stages of the adsorption process possess diverse mass transfer rates [62]. This implies that the intraparticle diffusion was not the only rate-limiting step in the sorption kinetics, and it can be concluded that both external mass transfer and intraparticle diffusion influence the adsorption process.

3.4 Isotherm studies

The experimental adsorption equilibrium data were investigated by using three important adsorption isotherms (Langmuir, Freundlich, and Temkin isotherm models) over the whole concentration range studied. These isotherms offer significant information about the adsorption capacity, binding mechanism, and surface characteristics of the adsorbent. Models fitting to experimental results are shown in Fig. 7a, b and c and Table 2. Based on the regression coefficient values (R^2) of the summarized data, it can be concluded that the Langmuir model has the highest value compared with the other models. These results show that the Langmuir model seems suitable for modeling the adsorption isotherms of MB on CMP surface. The results mean that the MB dye is adsorbed as a homogeneous monolayer on CMP surface. The obtained R_L value was 0.01 which confirms the favorability of MB dye adsorption under the experimental conditions

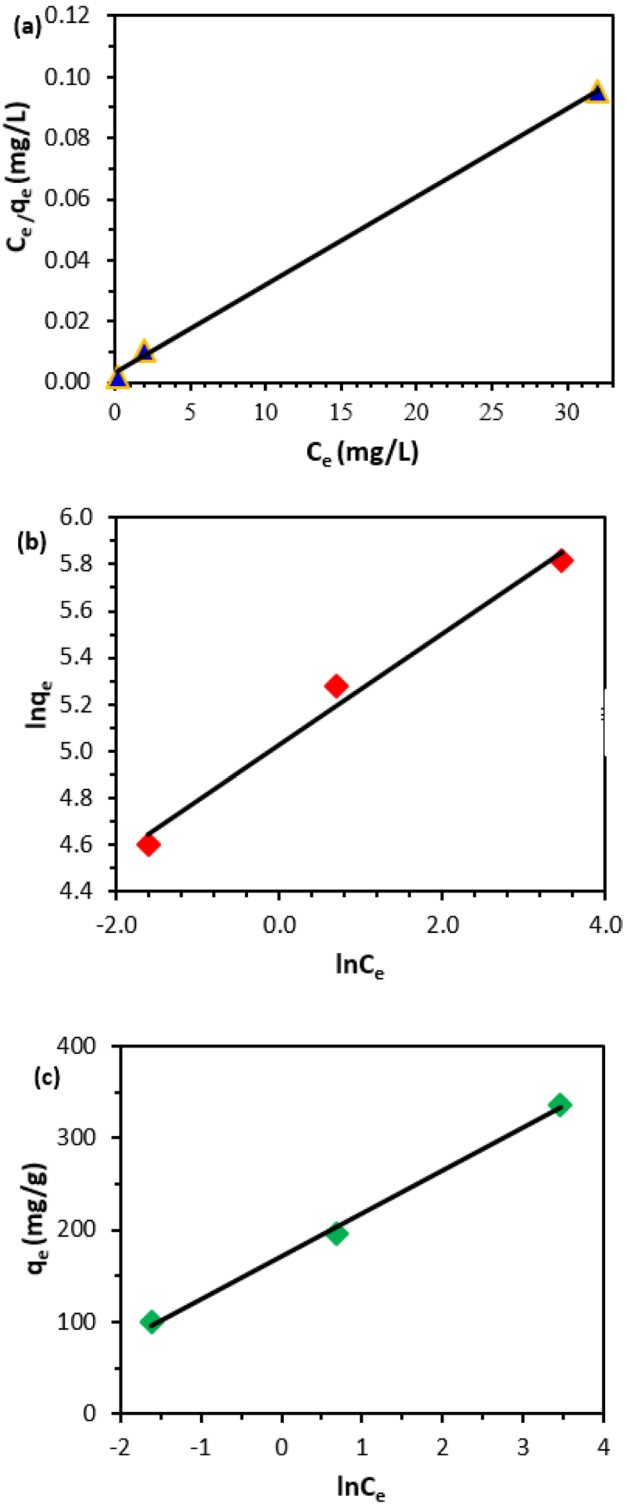

Fig. 7 The plot [Langmuir (**a**); Freundlich (**b**); Temkin (**c**)] isotherms for MB dye elimination over CMP, dosage = 0.01 mg, temperature = 298 K, pH = 6

Table 2 Parameters of isotherm models of MB dye removal by CMP

Langmuir			Freundlich				Temkin		
q_m (mg/g)	k_L (L/mg)	R^2	1/n	n	K_F (mg/g)	R^2	b_T (KJ/mol)	k_T (L/g)	R^2
345 ± 4	0.983	0.999	0.24	4.2	166	0.986	6.3	1	0.997

Table 3 Comparison of maximum adsorption capacity of MB dye with different composite materials from literature

Adsorbent	Adsorption capacity (mg/g)	References
Magnetic graphene oxide modified zeolite	82.1	[14]
Titania-incorporated polyamide	43	[50]
Co-polymer-grafted gum karaya and silica hybrid hydrogel	43.9	[63]
Polyaniline/zirconium oxide	77.5	[64]
Hydroxyapatite-sodium alginate	77.5	[65]
Reed biochar supported hydroxyapatite	17.5	[66]
Iron-based metal–organic framework	8.7	[67]
Hydrolyzed polyacrylamide modified diatomite waste	37.1	[68]
Zeolitic imidazolate framework-8	71.4	[69]
Single-walled carbon nanotubes-amine	136	[70]
Polyamide grafted on eggshell	345 ± 4	Present study

conducted in this study. The maximum adsorption capacity (q_m) of CMP composite is equal to 345 ± 4 mg/g. Table 3 displays the comparison of MB dye adsorption capacities with several adsorbents. The polyamide grafted on eggshell composite can be effectively used as an adsorbent for removing MB dye from an aqueous solution.

3.5 Simultaneous adsorption of metal ions and dye in a real water sample

There are many organic and inorganic pollutants in industrial effluents. The process of dye adsorption may be influenced by the existence of heavy metals, so it is essential to inspect

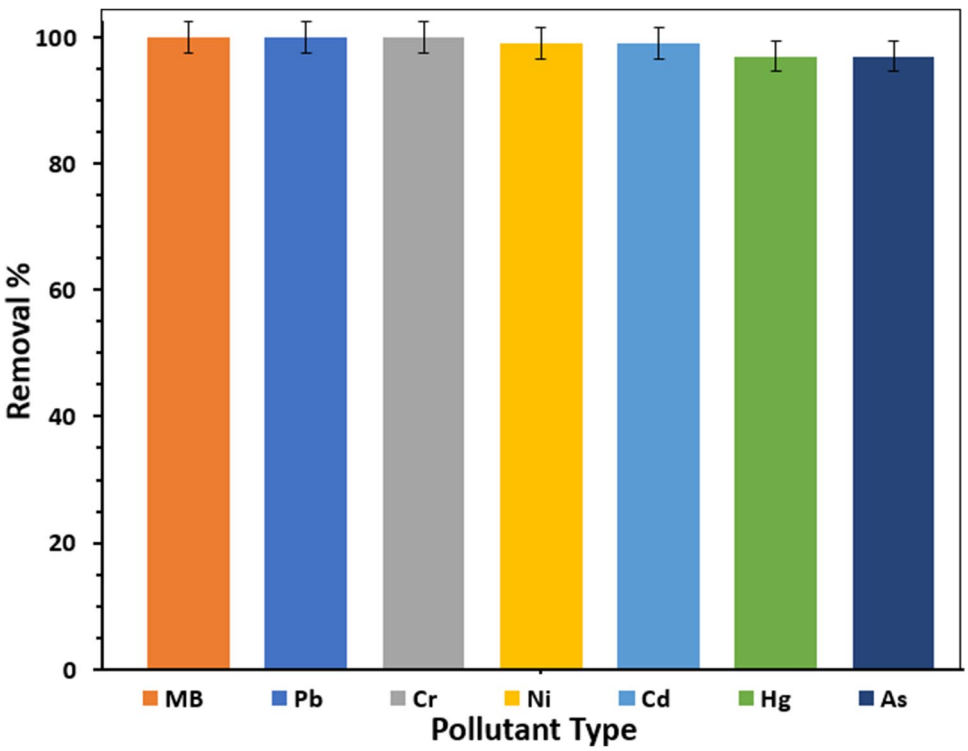

Fig. 8 Simultaneous removal of MB dye and toxic metals by CMP composite

the influence of the components. The water spiked with 100 ppm of methylene blue dye and lead, chromium, mercury, nickel, cadmium, and arsenic metal ions was treated with the prepared CMP composite. The results are shown in Fig. 8. The prepared CMP composite was efficient in simultaneous removal of both the dye and the metal ions with almost 100 percent removal of the dye, while the total removal of metal ions was more than 98%. The metal ion removal was high for the lead, chromium, nickel, and cadmium with ≈ 100% removal, while it was 97% removal for the mercury and arsenic. The obtained results indicate that the prepared adsorbent can be used for the treatment of real water. The adsorption capacity was not influenced by the simultaneous existence of the ME dye and the toxic metal ions. It is worth mentioning that the captured heavy metal ions can form an eggshell metal complex that can be further used to adsorb ME dye from aqueous solutions and cause the possible formation of multilayer adsorption [36]. Therefore, there are several types of interactions that could be involved in the adsorption which may describe the high adsorption of MB dye and the metal ions. Possible mechanisms could take place including the π-π interaction, the electrostatic interaction in addition to the complexation interaction between MB dye and metals.

3.6 Mechanism of adsorption of methylene blue dye and metal ions

Several mechanisms can be involved in the adsorption process. The adsorption mechanism of MB dye and metal ions on the surface of CMP through different types of interactions is displayed in Fig. 9. The π-π interaction can take place between the aromatic rings of MB dye and hexagonal skeleton of CMP. An electrostatic attraction can occur

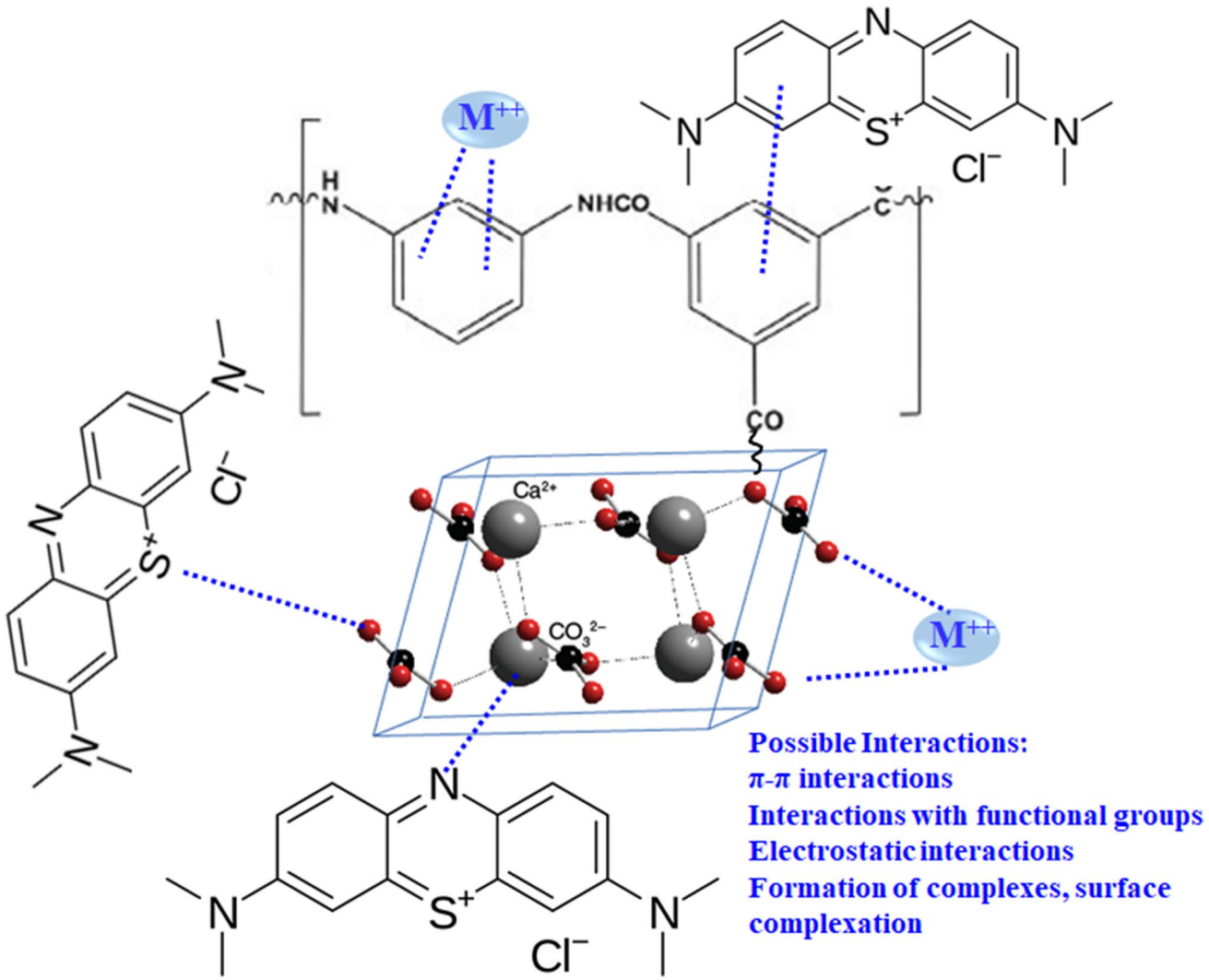

Fig. 9 Mechanisms of pollutants removal over CMP composite

between the positively charged molecules of MB dye and the negative charges that exist on the surface of CMP. Adsorption mechanism also occurs by the interaction between the cations of MB dye and functional groups that are available on the surface of CMP such as hydroxyl (OH), carbonyl (C = O), and carboxyl (COOH) groups as confirmed by FTIR analysis. Finally, complexation interaction can take place between MB dye and metal ions. Based on the above discussion, adsorption is a complex process, and it can be concluded that these interactions are effective in improving the adsorption of MB dye and metal ions on the surface of the CMP. Similar results were obtained by other studies for the MB dye adsorption on carbon nanotube [71] and coal-activated carbon [72].

4 Conclusions

The polyamide grafted eggshell composite (CMP) was successfully synthesized and applied for the removal of MB dye and metal ions from the aqueous solution. The maximum adsorption capacity was achieved under the conditions of an initial concentration of 200 ppm, the adsorbent dosage of 0.01 mg, and solution pH of 6 at room temperature. Kinetic studies were implemented to understand the adsorption mechanism. The kinetic and isotherm models data revealed that the pseudo-second-order model fitted the adsorption data. The adsorption capacity of the CMP was 345 mg/g at 298 K for MB dye. The adsorption mechanisms included π-π interactions, electrostatic attraction, interaction with functional groups, and formation of complexes. The CMP showed simultaneous removal of MB dye and toxic metals such as Pb, Cr, Ni, Cd, Hg, and As. The adsorption results revealed that the CMP is an efficient and low-cost biosorbent for the removal of MB dye and metal ions.

Acknowledgements The author TA Saleh thanks KFUPM, Saudi Arabia, for the support (Project No. DF201019).

Declarations

Conflict of interest The authors declare no competing interests.

References

1. Jack Clifton II, Leikin JB (2003) Methylene blue. Am J Ther 10:289–291
2. Lellis B, Fávaro-Polonio CZ, Pamphile JA, Polonio JC (2019) Effects of textile dyes on health and the environment and bioremediation potential of living organisms. Biotechnol Res Innov 3:275–290
3. Narwade VN, Khairnar RS, Kokol V (2018) In situ synthesized hydroxyapatite—cellulose nanofibrils as biosorbents for heavy metal ions removal. J Polym Environ 26:2130–2141
4. Moreno-Sader K, García-Padilla A, Realpe A, Acevedo-Morantes M, Soares JBP (2019) Removal of heavy metal water pollutants (Co2+ and Ni2+) using polyacrylamide/sodium montmorillonite (PAM/Na-MMT) nanocomposites. ACS Omega 4:10834–10844
5. Saleh TA (2020) Nanomaterials: classification, properties, and environmental toxicities. Environ Technol Innov 20:101067
6. Saleh TA (2021) Protocols for synthesis of nanomaterials, polymers, and green materials as adsorbents for water treatment technologies. Environ Technol Innov 24:101821
7. Saleh TA (2018) Simultaneous adsorptive desulfurization of diesel fuel over bimetallic nanoparticles loaded on activated carbon. J Clean Prod 172:2123–2132
8. Saleh TA (2020) Trends in the sample preparation and analysis of nanomaterials as environmental contaminants. Trends Environ Anal Chem 28:e00101
9. Mouni L, Belkhiri L, Bollinger J-C, Bouzaza A, Assadi A, Tirri A et al (2018) Removal of methylene blue from aqueous solutions by adsorption on Kaolin: kinetic and equilibrium studies. Appl Clay Sci 153:38–45
10 Saleh TA, Sarı A, Tuzen M (2002) Simultaneous removal of polyaromatic hydrocarbons from water using polymer modified carbon. Biomass Conv Bioref. https://doi.org/10.1007/s13399-021-02163-9
11. T.A. Saleh, M Mustaqeem, M Khaled, Water treatment technologies in removing heavy metal ions from wastewater: a review. Environ Nanotechnol Monit Manag :100617. https://doi.org/10.1016/j.enmm.2021.100617.
12. Saleh TA (2017) Insights into carbon nanotube-metal oxide composite: embedding in membranes, Int J Sci. Res Environ Sci Toxicol 2(1):1–4
13. Bin-Dahman OA, Saleh TA (2020) Synthesis of carbon nanotubes grafted with PEG and its efficiency for the removal of phenol from industrial wastewater. Environ Nanotechnol Monit Manag 13:100286
14. Saleh TA, Elsharif AM, Bin-Dahman OA (2021) Synthesis of amine functionalization carbon nanotube-low symmetry porphyrin derivatives conjugates toward dye and metal ions removal. J Mol Liq 340:117024
15. Sankaran R, Show PL, Ooi C-W, Ling TC, Shu-Jen C, Chen S-Y et al (2020) Feasibility assessment of removal of heavy metals and soluble microbial products from aqueous solutions using eggshell wastes, Clean Technol. Environ. Policy 22:773–786
16. Burakov AE, Galunin EV, Burakova IV, Kucherova AE, Agarwal S, Tkachev AG et al (2018) Adsorption of heavy metals on conventional and nanostructured materials for wastewater treatment purposes: a review. Ecotoxicol Environ Saf 148:702–712
17. Van Thuan T, Quynh BTP, Nguyen TD, Bach LG (2017) Response surface methodology approach for optimization of Cu2+, Ni2+ and Pb2+ adsorption using KOH-activated carbon from banana peel. Surfaces and Interfaces 6:209–217
18 Javadian H, Ruiz M, Saleh TA, Sastre AM (2020) Ca-alginate/carboxymethyl chitosan/Ni0. 2Zn0. 2Fe2. 6O4 magnetic bionanocomposite: Synthesis, characterization and application for single adsorption of Nd+ 3, Tb+ 3, and Dy+ 3 rare earth elements from aqueous media. J Mol Liq 306:112760
19. de Oliveira AP, Módenes AN, Bragião ME, Hinterholz CL, Trigueros DEG, G. de O. Isabella, (2018) Use of grape pomace as a biosorbent for the removal of the Brown KROM KGT dye. Bioresour Technol Rep 2:92–99
20. Tsai W-T, Hsien K-J, Hsu H-C, Lin C-M, Lin K-Y, Chiu C-H (2008) Utilization of ground eggshell waste as an adsorbent for the removal of dyes from aqueous solution. Bioresour Technol 99:1623–1629
21. Kyzas GZ, Lazaridis NK, Mitropoulos AC (2012) Removal of dyes from aqueous solutions with untreated coffee residues as

potential low-cost adsorbents: equilibrium, reuse and thermodynamic approach. Chem Eng J 189:148–159
22. El-Bindary AA, El-Sonbati AZ, Al-Sarawy AA, Mohamed KS, Farid MA (2014) Adsorption and thermodynamic studies of hazardous azocoumarin dye from an aqueous solution onto low cost rice straw based carbons. J Mol Liq 199:71–78
23. Hazzaa R, Hussein M (2015) Adsorption of cationic dye from aqueous solution onto activated carbon prepared from olive stones. Environ Technol Innov 4:36–51
24. Fernández-López JA, Angosto JM, Roca MJ, Miñarro MD (2019) Taguchi design-based enhancement of heavy metals bioremoval by agroindustrial waste biomass from artichoke. Sci Total Environ 653:55–63
25. Noreen S, Bhatti HN (2014) Fitting of equilibrium and kinetic data for the removal of Novacron Orange P-2R by sugarcane bagasse. J Ind Eng Chem 20:1684–1692
26. Zhang Y-J, Ou J-L, Duan Z-K, Xing Z-J, Wang Y (2015) Adsorption of Cr (VI) on bamboo bark-based activated carbon in the absence and presence of humic acid. Colloids Surf A Physicochem Eng Asp 481:108–116
27. Alhussary BN, Taqa GA, Taqa AAA (2020) Preparation and characterization of natural nano hydroxyapatite from eggshell and seashell and its effect on bone healing. J Appl Vet Sci 5:25–32
28. Tshizanga N, Aransiola EF, Oyekola O (2017) Optimisation of biodiesel production from waste vegetable oil and eggshell ash, South African. J Chem Eng 23:145–156
29. Bandhavya GB, Sandeep K, Bindhushree GB (2017) An experimental study on partial replacement of cement with egg shell powder in concrete. Int Res J Eng Technol 4:2017
30. Wazir A, Gul Z, Hussain M (2018) Comparative study of various organic fertilizers effect on growth and yield of two economically important crops, potato and pea. Agric Sci 9:703
31 Zaman T, Mostari M, Al Mahmood MA, Rahman MS (2018) Evolution and characterization of eggshell as a potential candidate of raw material. Cerâmica. 64:236–241
32. Cree D, Rutter A (2015) Sustainable bio-inspired limestone eggshell powder for potential industrialized applications. ACS Sustain Chem Eng 3:941–949
33. Carvalho J, Araújo J, Castro F (2011) Alternative low-cost adsorbent for water and wastewater decontamination derived from eggshell waste: an overview. Waste Biomass Valoriz 2:157–167
34. Al-Ghouti MA, Salih NR (2018) Application of eggshell wastes for boron remediation from water. J Mol Liq 256:599–610
35. Dayanidhi K, Vadivel P, Jothi S, Eusuff NS (2020) Facile synthesis of silver@ eggshell nanocomposite: a heterogeneous catalyst for the removal of heavy metal ions, toxic dyes and microbial contaminants from water. J. Environ. Manage. 271:110962
36. Zhang Y, Hong X, Cao X, Huang X, Hu B, Ding S, Lin H (2021) Functional porous organic polymers with conjugated triaryl triazine as the core for superfast adsorption removal of organic dyes. ACS Appl Mater Interfaces 13(5):6359–6366
37. Rezania H, Vatanpour V, Salehi E, Gavari N, Shockravi A, Ehsani M (2019) Wholly heterocycles-based polyamide–sulfide containing pyridine and thiazole rings: a super-adsorbent polymer for lead removal. J Polym Environ 27:1790–1800
38. Dotto GL, Santos JMN, Tanabe EH, Bertuol DA, Foletto EL, Lima EC et al (2017) Chitosan/polyamide nanofibers prepared by Forcespinning® technology: a new adsorbent to remove anionic dyes from aqueous solutions. J Clean Prod 144:120–129
39. Moradi E, Ebrahimzadeh H, Mehrani Z, Asgharinezhad AA (2019) The efficient removal of methylene blue from water samples using three-dimensional poly (vinyl alcohol)/starch nanofiber membrane as a green nanosorbent. Environ Sci Pollut Res 26:35071–35081
40. Saleh TA, Sarı A, Tuzen M (2021) Development and characterization of bentonite-gum arabic composite as novel highly-efficient adsorbent to remove thorium ions from aqueous media. Cellulose 28(16):10321–10333
41. Kango S, Kalia S, Celli A, Njuguna J, Habibi Y, Kumar R (2013) Surface modification of inorganic nanoparticles for development of organic–inorganic nanocomposites—a review. Prog Polym Sci 38:1232–1261. https://doi.org/10.1016/J.PROGPOLYMSCI.2013.02.003
42. Lagergren SK (1898) About the theory of so-called adsorption of soluble substances. Sven Vetenskapsakad Handingarl 24:1–39
43. Ho Y-S, McKay G (1999) Pseudo-second order model for sorption processes. Process Biochem 34:451–465
44. Weber WJ Jr, Morris JC (1963) Kinetics of adsorption on carbon from solution. J Sanit Eng Div 89:31–59
45. Langmuir I (1918) The adsorption of gases on plane surfaces of glass, mica and platinum. J Am Chem Soc 40:1361–1403. https://doi.org/10.1021/ja02242a004
46. Weber TW, Chakravorti RK (1974) Pore and solid diffusion models for fixed-bed adsorbers. AIChE J 20:228–238
47. Arami M, Limaee NY, Mahmoodi NM (2006) Investigation on the adsorption capability of egg shell membrane towards model textile dyes. Chemosphere 65:1999–2008
48. Freundlich HMF (1906) Over the adsorption in solution. J Phys Chem 57:1100–1107
49. Tempkin MI, Pyzhev V (1940) Kinetics of ammonia synthesis on promoted iron catalyst. Acta Phys Chim USSR 12:327
50. Ali I, S.A. AL-Hammadi, T.A. Saleh, (2018) Simultaneous sorption of dyes and toxic metals from waters using synthesized titania-incorporated polyamide. J Mo. Liq 269:564–571
51. Elzain AA, El-Aassar MR, Hashem FS, Mohamed FM, Ali ASM (2019) Removal of methylene dye using composites of poly (styrene-co-acrylonitrile) nanofibers impregnated with adsorbent materials. J Mol Liq 291:111335
52. Saleh TA (2015) Mercury sorption by silica/carbon nanotubes and silica/activated carbon: a comparison study. J Water Supply Res Technol 64:892–903
53. Abualnaja KM, Alprol AE, Abu-Saied MA, Mansour AT, Ashour M (2021) Studying the adsorptive behavior of poly (acrylonitrile-co-styrene) and carbon nanotubes (nanocomposites) impregnated with adsorbent materials towards methyl orange dye. Nanomaterials 11:1144
54. Sousa HR, Silva LS, Sousa PAA, Sousa RRM, Fonseca MG, Osajima JA et al (2019) Evaluation of methylene blue removal by plasma activated palygorskites. J Mater Res Technol 8:5432–5442
55. Qi C, Zhao L, Lin Y, Wu D (2018) Graphene oxide/chitosan sponge as a novel filtering material for the removal of dye from water. J Colloid Interface Sci 517:18–27
56. He J, Cui A, Deng S, Chen JP (2018) Treatment of methylene blue containing wastewater by a cost-effective micro-scale biochar/polysulfone mixed matrix hollow fiber membrane: performance and mechanism studies. J Colloid Interface Sci 512:190–197
57. Allen SJ, Koumanova B (2005) Decolourisation of water/wastewater using adsorption. J Univ Chem Technol Metall 40:175–192
58. Moreno-Castilla C (2004) Adsorption of organic molecules from aqueous solutions on carbon materials. Carbon N Y 42:83–94
59. Wong S, AbdGhafar N, Ngadi N, Razmi FA, Inuwa IM, Mat R et al (2020) Effective removal of anionic textile dyes using adsorbent synthesized from coffee waste. Sci. Rep. 10:1–13
60. Murcia-Salvador A, Pellicer JA, Rodríguez-López MI, Gómez-López VM, Núñez-Delicado E, Gabaldón JA (2020) Egg by-products as a tool to remove direct Blue 78 dye from wastewater: kinetic, equilibrium modeling, thermodynamics and desorption properties. Materials (Basel) 13:1262

61. El-Kemary MA, El-mehasseb IM, Shoueir KR, El-Shafey SE, El-Shafey OI, Aljohani HA et al (2018) Sol-gel TiO2 decorated on eggshell nanocrystal as engineered adsorbents for removal of acid dye. J Dispers Sci Technol 39:911–921
62. Saleh TA, Tuzen M, Sarı A (2018) Polyamide magnetic palygorskite for the simultaneous removal of Hg (II) and methyl mercury; with factorial design analysis. J Environ Manage 211:323–333
63. Mittal H, Maity A, Ray SS (2015) Synthesis of co-polymer-grafted gum karaya and silica hybrid organic–inorganic hydrogel nanocomposite for the highly effective removal of methylene blue. Chem Eng J 279:166–179. https://doi.org/10.1016/J.CEJ.2015.05.002
64. Agarwal S, Tyagi I, Gupta VK, Golbaz F, Golikand AN, Moradi O (2016) Synthesis and characteristics of polyaniline/zirconium oxide conductive nanocomposite for dye adsorption application. J Mol Liq 218:494–498
65. Guesmi Y, Agougui H, Lafi R, Jabli M, Hafiane A (2018) Synthesis of hydroxyapatite-sodium alginate via a co-precipitation technique for efficient adsorption of Methylene Blue dye. J Mol Liq 249:912–920
66. Li Y, Zhang Y, Wang G, Li S, Han R, Wei W (2018) Reed biochar supported hydroxyapatite nanocomposite: characterization and reactivity for methylene blue removal from aqueous media. J Mol Liq 263:53–63
67. Arora C, Soni S, Sahu S, Mittal J, Kumar P, Bajpai PK (2019) Iron based metal organic framework for efficient removal of methylene blue dye from industrial waste. J Mol Liq 284:343–352
68. Ma T, Wu Y, Liu N, Wu Y (2020) Hydrolyzed polyacrylamide modified diatomite waste as a novel adsorbent for organic dye removal: adsorption performance and mechanism studies. Polyhedron. 175:114227
69. Panda J, Sahoo JK, Panda PK, Sahu SN, Samal M, Pattanayak SK et al (2019) Adsorptive behavior of zeolitic imidazolate framework-8 towards anionic dye in aqueous media: combined experimental and molecular docking study. J Mol Liq 278:536–545
70. Maazinejad B, Mohammadnia O, Ali GAM, Makhlouf ASH, Nadagouda MN, Sillanpää M et al (2020) Taguchi L9 (34) orthogonal array study based on methylene blue removal by single-walled carbon nanotubes-amine: adsorption optimization using the experimental design method, kinetics, equilibrium and thermodynamics. J Mol Liq 298:112001
71. Zhang Z, Xu X (2014) Wrapping carbon nanotubes with poly (sodium 4-styrenesulfonate) for enhanced adsorption of methylene blue and its mechanism. Chem Eng J 256:85–92
72. Jawad AH, Ismail K, Ishak MAM, Wilson LD (2019) Conversion of Malaysian low-rank coal to mesoporous activated carbon: structure characterization and adsorption properties, Chinese. J Chem Eng 27:1716–1727